# Geochemistry of Panjal Traps from Zanskar Region: Implications for petrogenesis and geochemical variabilities

A Thesis

by

Sanket Samal
20226401


Indian Institute of Science Education and Research Pune
March, 2024

under the guidance of
**Dr. Gyana Ranjan Tripathy**
Department of Earth and Climate Science
IISER Pune

# Certificate

This is to certify that the dissertation titled *"**Geochemistry of Panjal Traps from Zanskar Region: Implications for petrogenesis and geochemical variabilities"*** submitted to the Department of Earth and Climate Science, towards the fulfilment of the M.Sc. (Geology) degree programme at the Indian Institute of Science Education and Research, Pune, represents a bonafide project carried out by **Sanket Samal** at IISER Pune under the supervision of **Dr. Gyana Ranjan Tripathy**, Associate Professor, Department of Earthand Climate Sciences, during the academic year 2023-2024. This report has not formed the basis for award of any Degree/Diploma/Associateship/Fellowship or any similar title to any candidate of any university.

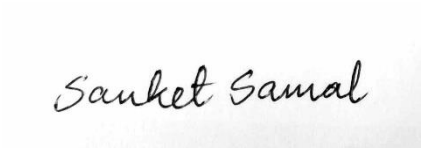

Sanket Samal
(M.Sc. Student)

Dr. Gyana Ranjan Tripathy
(Supervisor)

# Declaration

I hereby declare that the research work presented in the report entitled *"**Geochemistry of Panjal Traps from Zanskar Region: Implications for petrogenesis and geochemical variabilities"*** have been carried out by me at the Department of Earth and Climate Sciences, Indian Institute of Science Education and Research, Pune under the supervision of Dr. Gyana Ranjan Tripathy and the same has not been submitted elsewhere for any degree.

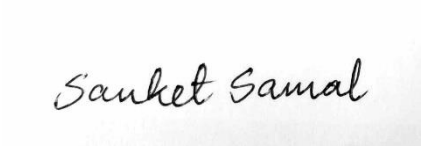

Sanket Samal
(M.Sc. Student)

Dr. Gyana Ranjan Tripathy
(Supervisor)

# Acknowledgement

I would like to express my sincere gratitude to the following individuals and organizations who have supported and helped me throughout my dissertation at IISER Pune.

First and foremost, I would like to thank my supervisor, Dr. Gyana Ranjan Tripathy, for his guidance, support, and encouragement throughout my research work. His expertise and feedbacks have been invaluable in shaping my ideas and improving the quality of my work.

I extend my sincere gratitude to Dr. Suraj Parcha from Wadia Institute of Himalayan Geology, as well as Anirban Mandal, Anupam Samanta, and Mohd Danish from IISER Pune, for their invaluable assistance during the field trip aimed at collecting the Zanskar samples.

This thesis could not have been successful without the constant support and guidance of Achyuth Venugopal. I appreciate all the hard work and sincerity he gave towards teaching me and helping me with the analyses to finish this research project well ahead of time. I am deeply indebted to him and my lab seniors Rakesh Kumar Rout, Kruttika Mohapatra and my fellow colleagues Samarpan Mahato and Raniria Mitra for their friendly demeanor and inclusive attitude which made me feel an integral part of the GRASP Lab. Their expertise and knowledge of the subject have helped me to refine my research and their dedication to scientific inquiry have been an inspiration to me.

# Contents

# List of Figures

# List of Tables

# Abstract

The Panjal Trap represents one of the largest outcrops of early Permian Period (~290Ma) volcanism associated with the separation of Cimmeria from Gondwana and opening of the Neothethys Ocean. In the Indian sector, these rocks are exposed in the Northern Himalayas along the Pir Panjal and Zanskar mountain ranges. While existing studies have provided detailed geological understanding of these volcanisms, few studies examine the geochemical variations associated with them. This thesis undertakes a geochemical study of the Panjal Traps from the less explored south-eastern Zanskar region to investigate regional variations in composition, petrogenesis and tectonics. The samples collected from the Zanskar region can be classified into basalts, basaltic trachyandesites, and trachyandesites of predominantly calc-alkaline composition. The observed enrichment of Light Rare Earth Elements (LREEs), uniform distribution of Heavy Rare Earth Elements (HREEs), along with elevated Nb/U, Nb/La, and $Th/Nb_{PM}$ ratios suggest a shallow spinel peridotite source for these melts. Pearce Elemental Ratios and elemental variations show occurrence of olivine-driven fractionation processes in the parental magma and minimal crustal assimilation. Tectonomagmatic diagrams suggests that the eruption occurred within an oceanic ridge setting, displaying chemical characteristics similar to Enriched Mid-Ocean Ridge Basalts (E-MORB). These findings are consistent with previous studies on Panjal Traps in the Kashmir Valley, signifying their geological linkage with the North eastern counterparts.

# 1. Introduction

Continental Large Igneous Provinces (LIPs) are represented by large scale deposition of mantle-derived volcanic rocks and their intrusive equivalents deposited over a time span of around 10-15 million years (Bryan & Ernst, 2008; Campbell, 2007). Various modes have been proposed for the generation of LIPs which include (i) the upwelling of mantle material originating from the core-mantle boundary (ii) decompression related mantle melting associated with tensional plate stress (the 'plate' model; Richards et al., 1989), and (iii) fluid induced melting occurring along convergent boundaries (Anderson & Natland, 2005; Ernst, 2014; Foulger, 2010). Such rapid emplacement of predominantly mafic magmas characteristic of LIPs often produces massive outpouring, which correlate with mass extinction, large scale tectonic changes and expulsion of huge amount of greenhouse gasses. Such events help in explaining both the long-term thermal conditions of the lithosphere, plate dynamics, as well as their impact on ecosystems (Schootbrugge & Wignall, 2016; Saunders et al., 2007; Rampino & Stothers, 1988). Understanding the formation and implications of LIPs, hence, is an active area of research necessitating a multidisciplinary approach.

The late Paleozoic era (~300-251 Ma) was marked by the peak of supercontinent Pangea and two large scale mass extinction events during the middle to late Permian (Guadalupian–Lopingian) (Wignall, 2001). The opening of the Neotethys Ocean caused Pangea to divide, resulting in the formation of several Peri-Gondwana continental blocks from northeastern Gondwana (Stojanovic et al. 2016). The southern edges of this ocean included the northern rims of the Arabian, African, Australian and Indian plates (Stampfli et al., 1991; Dercourt et al., 1993) which formed as passive margins during the Mesozoic. The remnants of those marginal plate boundaries bear evidence for several intraplate magmatic occurrences across the Tethyan orogenic region such as the Himalayas, Oman, Australia and the Zagros and eastern Mediterranean ranges including Turkey and Cyprus (Maury et al., 2008). Notably, this period also saw the emplacement of at least five major LIPs, including the Himalayan magmatic province along the Tethyan margin of Gondwana (~290-270 Ma), Skagerrak-cantered LIP in central Laurasia (~300 Ma), the Tarim LIP near the Tethyan margin of Laurasia (~290-270 Ma), the Emeishan LIP of the South China Block (~260 Ma), and the Siberian Traps of NE Laurasia (~251 Ma; Saunders & Reichow, 2009; Shellnutt, 2014; Torsvik et al., 2008; Timmerman et al., 2009; Zhu et al., 2010; Yang et al., 2013; Wang et al., 2014). Collectively, these LIPs covered an area exceeding 7 million square kilometers with massive outcrops dominated by mafic volcanic and intrusive rocks (Shellnut, 2017).

In contrast, the late Paleozoic LIPs are largely unassociated with plate separation processes (Shellnutt, 2014; Torsvik et al., 2008). Among these Late Paleozoic LIPs, the Himalayan magmatic province (HMP) represents a unique case, being temporally linked with plate separation. The HMP encompasses a diverse assemblage of volcanic, plutonic sequences, and mafic outcrops that broadly coincide with the rifting of microcontinental terranes from the Tethyan margin of Gondwana and evolution of Cimmeria (Papritz & Rey 1989; Bhat et al. 1981; Yan et al. 2005; Zhu et al. 2010; Wang et al. 2014; Zhai et al. 2013; Shellnutt et al. 2014). The exact petrogenetic connection among the diverse volcanic and plutonic rocks constituting the Himalayan magmatic province (HMP) remains uncertain. Various Permian volcanic sequences found in the central and eastern Himalayas, including the Abor, Nar-Tsum, Selong, Mojiang and Bhote Kosi volcanic groups along the eastern extension of Himalayas, alongside the Qiangtang mafic dykes in China, are considered associated with the formation of the Neotethys Ocean and the Cimmeria continent (Sengör 1987; Yan et al. 2005; Zhu et al. 2010; Wang et al. 2014; Zhai et al. 2013). Studies also suggest that the HMP could also represent a compilation of distinct and independent units, potentially emplaced within the same regional-scale tensional regime during the early Permian epoch (Shellnut., 2017).

The Panjal Traps, situated in the western Himalayas of India and Pakistan, constitute the one of the major exposed outcrop of the HMP, yet their origins and formation remain unclear. Panjal Traps occur in the Pir Panjal and Zanskar mountain ranges of Kashmir, with correlative units observed in other regions of the western Himalayas as well. Originally believed to be of Upper Palaeozoic age, in situ zircon U–Pb yielded an age of close to lower Permian (289 ± 3 Ma; Shellnutt et al., 2011). Geochemical analyses of the Traps suggest similarities with within-plate continental tholeiites, related to the opening of the Neotethys Ocean (Chauvet et al. 2008; Shellnutt et al., 2014, 2015). Studying the Panjal Traps is crucial for unraveling the collision tectonics of Gondwana and the creation of one of the rare late Paleozoic 'plate-separation' mafic continental flood basalt provinces. It also offers valuable insights into the geodynamic and tectono-magmatic evolution of the late Permian Tethyan margin of Gondwana, shedding light on the formation of Large Igneous Provinces (LIPs) and their origins. The Panjal lava occurrences have been unevenly researched in terms of their geochemical features, with linkages established between the various Permian Traps outcrops. This thesis focuses on the less explored Zanskar region (NW Himalayan volcanics) to get more insights on the volcanic events co-incident with the rifting of the northern Indian plate during the late Permian.

# 2. Geological Background

The Tethyan sector of the western Indian Himalaya encompasses a geological assemblage spanning from Precambrian to Late Palaeozoic (Wadia 1934, 1961). The bedrock is comprised of Precambrian crystalline basement, including augen nebulitic migmatites, granitic gneisses, and various paragenetic rock, forming the basement of the passive margin deposits of the Tethyan sedimentary strata. These sedimentary sequences, ranging from Cambrian to Lower Carboniferous periods, is composed of, shale, siltstone, sandstone carbonate, and evaporite lithologies spread over the entire Himalayan Phanerozoic outcrops (Gaetani et al. 1986; Brookfield et al. 2013; Fuchs 1987). The Panjal Traps include volcanic successions outcropping in the north western Himalayas (near Kashmir valley, Lahul, Spiti, Zanskar) and parts of Pakistan (Honegger et al., 1982; Spencer et al., 1995; Papritz and Rey, 1989). The Middle–Upper Carboniferous Fenestella shale, bearing the index fossil *Spirifer varuna* and *Camarophoria* fossils, transitions into the fossiliferous Agglomeratic slate, marking the initial eruptive phase of the Panjal Traps. The main volcanic succession of the Panjal Traps erupted onto the Upper Permian siliciclastic Nishatbagh beds, superimposed over the Agglomeratic slate (Nakazawa et al. 1975; Garzanti et al. 1998; Wopfner & Jin 2009). The reported thickness of the volcanic rocks in the Pir Panjal Range in Kashmir valley approximate ~3000 m, contrasting with lesser thicknesses, around or less than ~300 m, in the Zanskar Range. Typically, individual flow units exhibit a thickness of approximately 30m over some section of Lahul-spiti sections (Chauvet et al. 2008; Nakazawa et al. 1975). The Panjal Traps are overlain by the Gangamopteris beds, housing fossils such as *Gangamopteris kasmirensis*, index fossil of an Upper Permian age. Subsequent sedimentary deposits include the Zewan Formation, characterized by carbonates and sandstones, overlain by the shales of upper Permian to Lower Triassic Khunamuh Formation (Wopfner & Jin 2009).

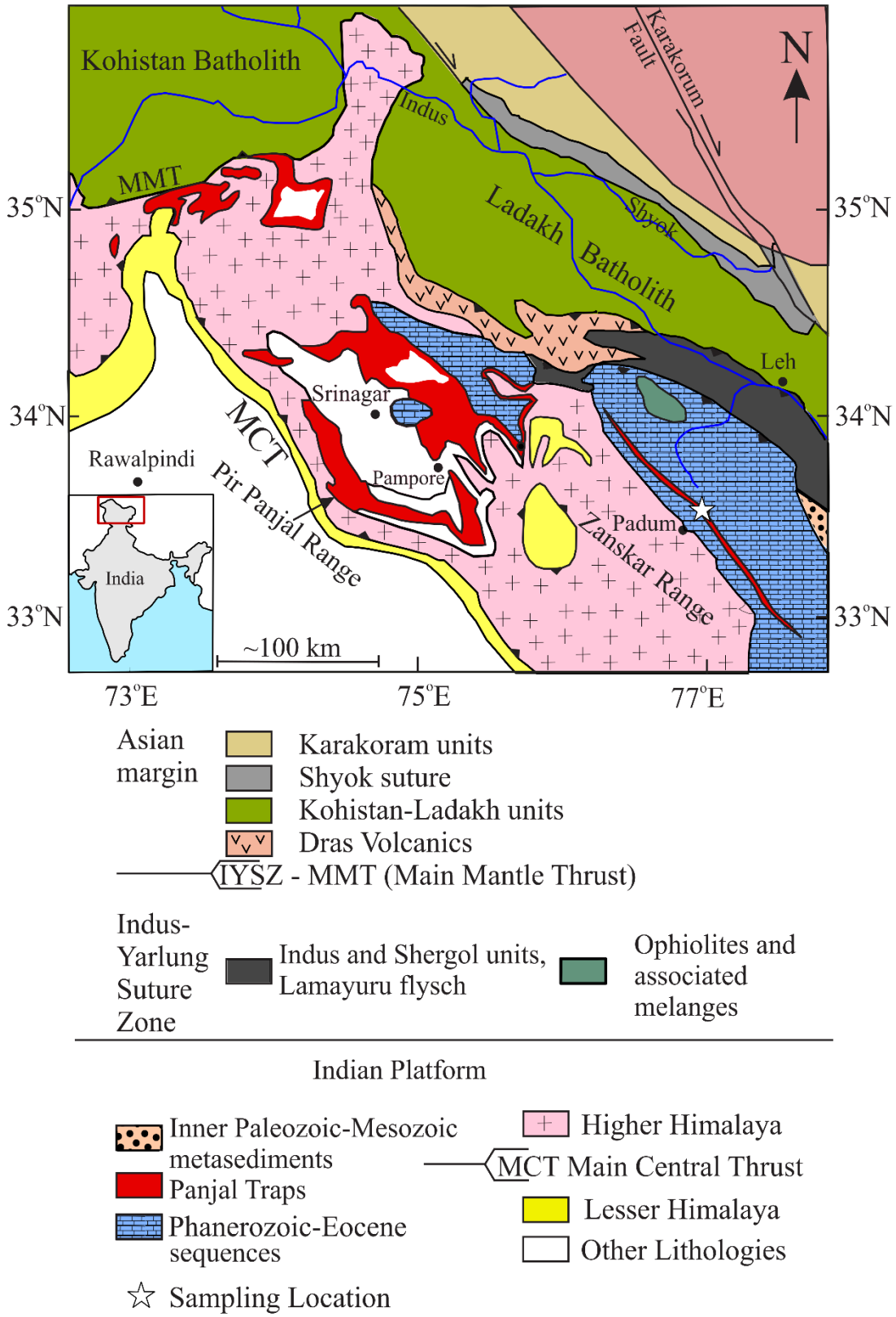


**Figure 1.** Geological map of the Panjal Traps in northern India and Pakistan (modified after Chauvet et al. (2008).

Encompassing an area of approximately 10,000 $km^2$, the Panjal Traps mainly consists of basalts, with minor occurrences of basaltic andesite, andesite, trachybasalt, rhyolite, and dacite (Bhat et al. 1981; Shellnutt et al. 2014). The volcanic formations are represented by the Agglomerate slate containing massive volcanic unit of ash and volcanic bombs, along with non-volcanic fossiliferous materials. The volcanic setting reveals evidence of both subaerial and subaqueous eruptive environments, suggesting a near-shore, transgressive shallow-marine setting (Spring and Vannay, 1933). The occurrence of intertrappean limestone, shales, and slates near Gulmarg and Bren suggests intermittent pauses during volcanic activity. Chemo-stratigraphic analyses have identified lateral variations in basalts along the vertical section within volcanic sequences from the western Kashmir Valley (Shellnutt et al. 2014). The inferred volcanic center of the Panjal Traps is situated in western Kashmir, notably within the Kashmir Valley where these outcrops show maximum stratigraphic thickness. The silicic volcanic rocks are found below the earliest basalt flows while the andesites are found at certain eruptive horizons within the major basaltic sequences of the Kashmir Valley (Shellnutt et al., 2012; Pareek 1976). The Panjal Traps are also associated with the Permian basalts and komatiites of Chhongtash in northern Ladakh (Rao and Rai., 2007).

The age of the Panjal volcanism has been a subject of great debate with initial inferences on the timing and duration of the Panjal Traps volcanic activity inferred from geological evidence. Middlemiss (1910) proposed an Upper Palaeozoic age based on the presence of fossiliferous presence of Ophiceras in overlying sediments. Detailed studies by Kapoor (1977) and Nakazawa et al. (1975) revealed that the lava flow occurred between the Late–Middle Carboniferous Fenestella shale deposition and Gangamopteris beds, implying an emplacement age no older than the Late Carboniferous. Carbonate rocks of Early Permian (Artinskian) age cap the basalts at Guryal Ravine. White (2002) and White & Saunders (2005) suggested a linkage with the mid-Capitanian mass extinction, implying an age of ~260 Myr.

Veevers & Tewari (1995) proposed correlation with Late Permian magmatic rocks (~250 Ma) along the Gondwana margin post-Neotethys Ocean opening. An eruption timeframe during the Kungutian–Artinskian period (275–258 million years ago) was suggested by Noble et al. (2001) Vannay & Spring (1993). U-Pb dating of the silicic Traps from Srinagar have yielded an age of 289 ± 3 Ma (Shellnut et al., 2007), which was consistent with the geological interpretation of Nakazawa et al. (1975). Previous reports of U-Pb zircon ages of the Yunam A-type granite in the Zanskar Valley yielded an age of 284 ± 1 Ma (Spring et al., 1993). Horton (2011) later reported U-Pb zircon age of 284 ± 4 Ma (LA-ICP-MS U–Pb) separated from granites of the Zanskar Valley, indicating extensive plutonic magmatism concurrent with the

Panjal volcanism. An eruption duration of 2-3 Myrs were proposed by Gaetani et al. (1990) based on faunal indicators from north-west Lahul–SE Zanskar.

# 3. Objective

The objective of this work is to determine the geochemical characteristics and magma source characteristics of Panjal Traps exposed in the Zanskar Region. This dataset is compared with other co-eval Panjal flows of the NW Himalayas (Guryal and Phalgham, Kashmir) and SE Himalayas (Lahul and Spiti) to provide an account for the lateral variations and geodynamic implications for the Panjal volcanism.

# 4. Analytical Methodology

Major and trace elemental composition of Pranjal traps samples have been measured following the analytical protocol of Samanta et al. (2022) (Figure 2.). Fresh basalt samples (n = 12) were collected from an outcrop (N 33° 31.211, E 76°59.426) from the Zanskar Valley in the NW Himalaays. About 100 g of rock samples were broken into ~2 cm chips, cleaned with MQ water and dried at ~60°C in an a hot air oven. The chips were powdered to <100 microns using an agate mortar and pestle. The powder was mixed thoroghly using coning and quartering method to enusre proper homogenity. The powder was then stored in airtight sample containers for further geochemical analysis.

For Major oxides concentrations, a known amount of sample (~0.55g) was mixed with Lithium Tetraborate-metaborate flux in a fixed ratio of 1:17 in a platinum crucible and fused at 1100°C. The major element concentrations of the fusion bead was analyzed using a wavelenghth-dispersive x-ray fluorescence spectrometer (Bruker S8 Tiger). The analysis was carried out using GEOQUANT Advanced calibration which is suitable for measuring the elemental oxide concentrations of geological materials. The accuracy of this analysis (±1%) was ensured by analysing USGS rock standards BCR-2, BHVO-2 and SGR-1b. Repeat analysis of samples yielded a reproducibility better than 1% for all oxides. For the determination of Loss on Ignition (LOI) of the samples, ~2 g of the powdered were combusted at 950°C, and the LOI was determined from the weight loss.

For trace elements, a known amount of samples was completely dissolved by treatment

with HF-$HNO_3$-HCl acids on a hotplate, heated at 130°C. The dissolved samples in 0.32N $HNO_3$ medium were filtered and stored in precleaned vials. The solutions were diluted (~500 times) and measured for elemental concentrations using a Q-ICPMS instrument in a Kinetic Energy Discrimination (KED) mode, which is a type of mode which reduces poly-atomic interferences. Two certified reference materials USGS BCR-2 and BHVO-2 were also processed and measured to monitor the accuracy and precision of the analysis.

We have used the major oxides data to compute the chemical index of alteration (CIA), which serves as a good proxy for degree of chemical weathering. The CIA values for these basalt samples were determined using the following equation, provided by (Nesbitt and Young, 1982).

$$CIA\ (in\ \%) = \frac{Al_2O_3}{Al_2O_3 + Na_2O + K_2O + CaO^*} \times 100$$

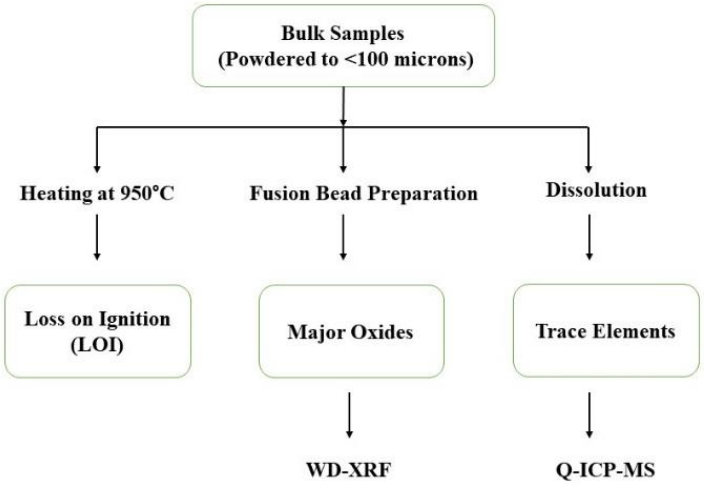


**Figure 2**. Flow chart of all the analytical methodology followed in this study

# 5. Results

Geochemical data for the Zanskar samples are given in Tables 1, 2 and 3. The $SiO_2$ concentrations of the samples range from 46.8 to 50.8 wt%. The Chemical Index of Alteration (CIA) values of these samples vary between 51.4% and 62.1%. This range is slightly higher than those expected for fresh basalt (30-45; Chen et al., 2023). The loss on ignition (LOI) values of these samples range from 1.8 to 4.1 wt% and rock textures of all samples indicate minimal post-depositional alterations. The Mg# ((evaluated as $(Mg^{2+}/(Mg^{2+}+Fe^{2+})) \times 100$) range from 34 to 46 (Table.1). Samples ZK-18-01, ZK-18-02, ZK-18-03, and ZK-18-04 have higher MgO content and lower CaO values compared to the rest of the samples, while samples ZK-18-09 and ZK-18-11 show high FeO content than the rest of the group. However, most of the samples fall in the range of basalts and basaltic trachyandesites with high compositional similarity. Samples ZK-18-1 and ZK-18-03 show chemical similarity, and show low CaO (~4.8 and ~ 4.6 wt%) and low $Na_2O + K_2O$ values (~4.1 and ~4.3 wt%). In comparison, samples ZK-18-05, ZK-18-06, ZK-18-07, and ZK-18-08 have higher CaO (~8.1 and ~ 8.4 wt%) and high alkali contents (~4.1 to ~5.2 wt%). The $TiO_2$ contents of these samples vary from ~0.8% to ~ 2.1 wt%, but their Mg# values are similar (34.8% to 36.3%).

The trace element composition of the basalts, basaltic trachyandesites, and trachybasalts are similar for the transition metals and high field strength elements (HFSEs). However, they show large variations in their large ion lithophile elements (LILE) compositions. The transition elements (Sc = 45-61 µg/g, V = 329-398 µg/g, Cr = 221-279 µg/g and Co = 51-65 µg/g) show variability, with sample ZK-18-12 showing depleted values while ZK-18-03 is highly enriched. The LILE elements (Rb = 16-82 µg/g, Ba = 136-428 µg/g, and Sr = 108-390 µg/g) are more variable, with Basaltic trachyandesites having more Rb, Ba, and Sr than the basalts. The high field strength (HFS) elements (Zr = 34-46 µg/g, Hf = 1.6-2.2 µg/g, Nb = 8.3-10 µg/g, U = 0.2-0.4 µg/g and Th = 1.7-2.2 µg/g) are the least variable elemental group. The patterns of primitive mantle normalized (PM; Sun and McDonough, 1989) incompatible trace element of the basalts, basaltic trachyandesites, and trachybasalts are similar (Figure. 3a). Both these rock types are enriched in LILEs relative to the HFSEs (Figure. 3b). They also show negative Ba, P, Zr, and Sr anomalies, LREE enrichment and negative Nb anomalies when normalized to Primitive Mantle (La/Nb from 1.0 to 1.6). Additionally, U shows enrichment throughout the samples. The primitive mantle normalized REE patterns (Figure 3b) also show a flat trend with LREE enrichment relative to MREE ($(La/Gd)_N$ between 1.1 and 1.7) and HREE ($(La/Yb)_N$ from 3.5 to 5.2).

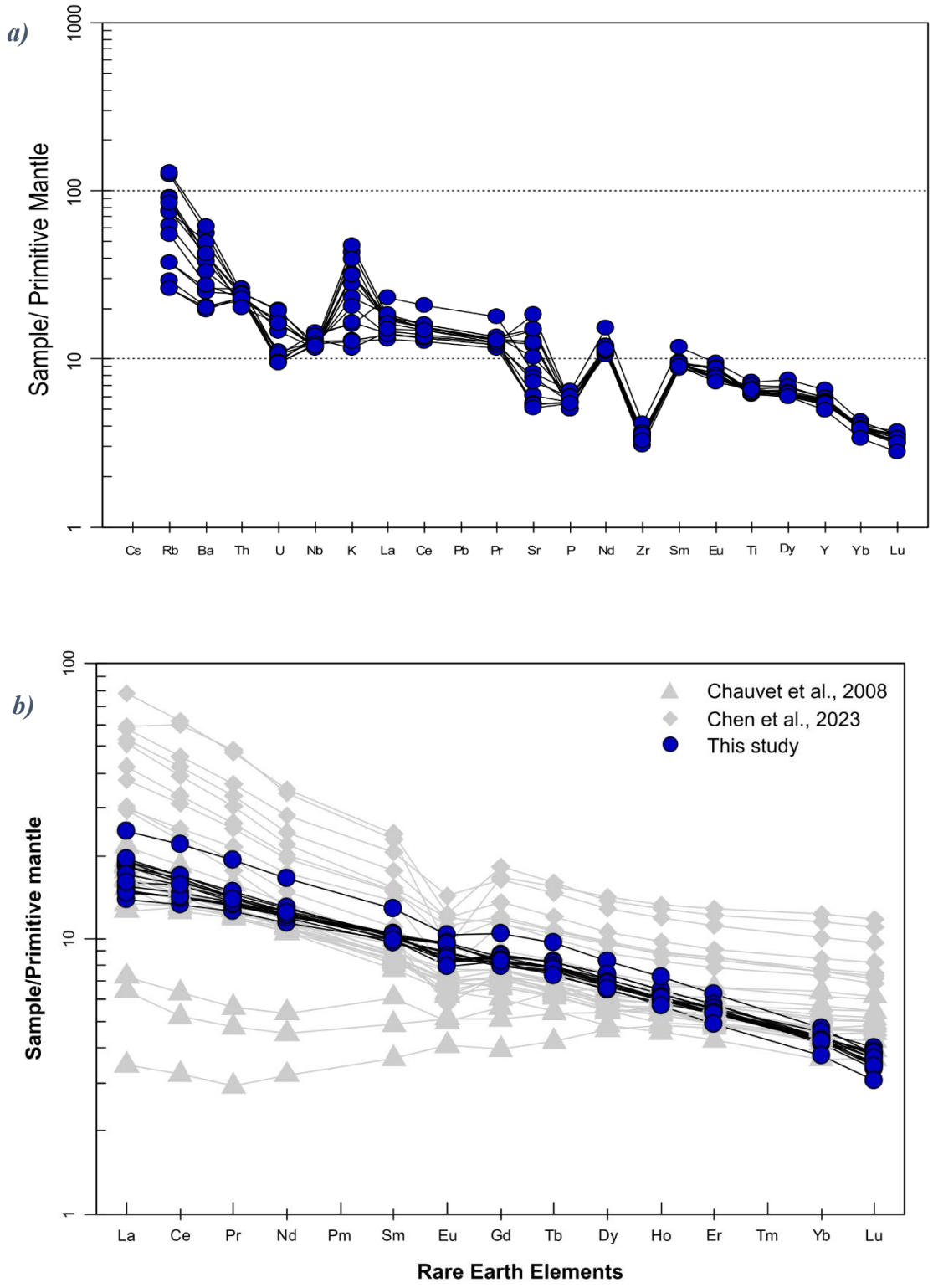


**Figure. 3:** Primitive mantle-normalized (a) incompatible elements (b) Rare Earth elements plot. The samples are normalized to Sun and McDonough (1989)

**Table -1** :- Major oxide and LOI data of Panjal Traps from Zanskar

| Sample ID | Sum (%) | LOI % | $Na_2O$ | MgO | $Al_2O_3$ | $SiO_2$ | $P_2O_5$ | $SO_3$ | $K_2O$ | CaO | $TiO_2$ | $Mn_2O_3$ | $Fe_2O_3$ |
|---|---|---|---|---|---|---|---|---|---|---|---|---|---|
| ZK-18-01 | 99.66 | 4.19 | 3.76 | 11.43 | 15.14 | 46.87 | 0.12 | 0.01 | 0.35 | 4.88 | 1.38 | 0.24 | 11.881 |
| ZK-18-02 | 99.40 | 3.83 | 3.60 | 10.96 | 14.44 | 47.35 | 0.14 | 0.01 | 0.48 | 5.76 | 1.58 | 0.23 | 11.574 |
| ZK-18-03 | 99.58 | 3.98 | 3.97 | 11.04 | 14.99 | 47.66 | 0.12 | 0.01 | 0.39 | 4.69 | 1.45 | 0.23 | 11.596 |
| ZK-18-04A | 99.73 | 3.77 | 4.09 | 10.98 | 14.47 | 48.57 | 0.12 | 0.01 | 0.38 | 5.14 | 1.40 | 0.24 | 11.092 |
| ZK-18-04B | 99.46 | 3.87 | 3.72 | 10.80 | 14.67 | 47.56 | 0.12 | 0.01 | 0.50 | 5.47 | 1.50 | 0.22 | 11.574 |
| ZK-18-05 | 99.44 | 2.04 | 4.12 | 7.09 | 14.15 | 50.57 | 0.11 | 0.01 | 0.96 | 8.19 | 1.35 | 0.19 | 11.168 |
| ZK-18-06 | 99.34 | 2.16 | 4.01 | 7.40 | 14.43 | 49.97 | 0.11 | 0.01 | 0.84 | 8.09 | 1.35 | 0.21 | 11.273 |
| ZK-18-07 | 99.37 | 1.89 | 4.28 | 6.77 | 14.31 | 50.77 | 0.11 | 0.01 | 0.96 | 8.44 | 1.34 | 0.15 | 10.81 |
| ZK-18-08A | 97.33 | 2.16 | 3.85 | 7.25 | 14.32 | 48.77 | 0.11 | 0.01 | 1.30 | 7.54 | 1.36 | 0.17 | 10.972 |
| ZK-18-08B | 98.51 | 2.06 | 3.67 | 6.92 | 14.39 | 49.41 | 0.12 | 0.01 | 1.42 | 8.28 | 1.40 | 0.19 | 11.158 |
| ZK-18-09 | 98.39 | 3.14 | 3.73 | 8.82 | 14.60 | 47.11 | 0.13 | 0.01 | 0.70 | 6.89 | 1.40 | 0.23 | 12.249 |
| ZK-18-10 | 98.72 | 3.46 | 3.50 | 7.35 | 14.63 | 48.43 | 0.12 | 0.01 | 0.95 | 8.10 | 1.37 | 0.23 | 11.086 |
| ZK-18-11 | 98.39 | 3.54 | 3.79 | 9.47 | 14.50 | 46.95 | 0.13 | 0.01 | 0.62 | 5.99 | 1.45 | 0.23 | 12.328 |
| ZK-18-12 | 99.45 | 2.76 | 4.04 | 8.40 | 14.40 | 50.57 | 0.12 | 0.01 | 1.18 | 6.42 | 1.42 | 0.23 | 10.342 |
| **Average** | 99.1 | 3.1 | 3.9 | 8.9 | 14.5 | 48.6 | 0.1 | 0.0 | 0.8 | 6.7 | 1.4 | 0.2 | 11.4 |
| **Std** | 0.7 | 0.9 | 0.2 | 1.8 | 0.3 | 1.4 | 0.0 | 0.0 | 0.4 | 1.4 | 0.1 | 0.0 | 0.5 |
| **Min** | 97.3 | 1.9 | 3.5 | 6.8 | 14.1 | 46.9 | 0.1 | 0.0 | 0.3 | 4.7 | 1.3 | 0.2 | 10.3 |
| **Max** | 99.7 | 4.2 | 4.3 | 11.4 | 15.1 | 50.8 | 0.1 | 0.0 | 1.4 | 8.4 | 1.6 | 0.2 | 12.3 |

**Table -2** :- Trace elements data of Panjal Traps from Zanskar region

| Sample ID | Rb | Sr | Zr | Hf | Y | Co | Cr | Ni | V | Sc | Cs | U | Nb | Ta | Ba | Th |
|---|---|---|---|---|---|---|---|---|---|---|---|---|---|---|---|---|
| | | | | | | | | | µg/g | | | | | | | |
| ZK-18-01 | 16.7 | 127.4 | 39.8 | 2.0 | 26.4 | 64.8 | 258.4 | 79.5 | 371.9 | 54.0 | 1.1 | 0.2 | 9.3 | 0.6 | 136.6 | 2.0 |
| ZK-18-02 | 23.9 | 174.5 | 46.1 | 2.2 | 29.7 | 62.3 | 279.8 | 83.6 | 392.3 | 61.1 | 1.3 | 0.2 | 10.2 | 0.7 | 182.3 | 2.2 |
| ZK-18-03 | 18.5 | 114.9 | 36.8 | 1.9 | 26.6 | 59.2 | 249.2 | 76.8 | 371.1 | 53.6 | 1.2 | 0.2 | 9.1 | 0.6 | 142.9 | 2.0 |
| ZK-18-04A | 16.7 | 112.8 | 40.7 | 2.0 | 25.4 | 53.7 | 243.1 | 72.3 | 361.7 | 51.5 | 1.2 | 0.2 | 8.7 | 0.6 | 140.5 | 1.9 |
| ZK-18-04B | 23.9 | 162.5 | 40.2 | 2.0 | 26.8 | 59.5 | 262.8 | 77.9 | 387.8 | 56.9 | 1.4 | 0.2 | 9.8 | 0.6 | 176.0 | 2.1 |
| ZK-18-05 | 58.4 | 266.5 | 39.3 | 1.8 | 25.2 | 51.6 | 231.5 | 70.7 | 384.3 | 51.1 | 3.4 | 0.3 | 8.6 | 0.6 | 290.6 | 2.0 |
| ZK-18-06 | 48.4 | 314.8 | 38.5 | 1.8 | 24.2 | 53.5 | 222.6 | 70.1 | 363.7 | 49.2 | 2.5 | 0.4 | 8.3 | 0.6 | 285.9 | 2.1 |
| ZK-18-07 | 57.4 | 255.2 | 39.7 | 1.8 | 24.3 | 46.7 | 219.1 | 66.6 | 365.3 | 47.4 | 3.1 | 0.4 | 8.3 | 0.5 | 265.7 | 1.9 |
| ZK-18-08A | 79.0 | 262.7 | 37.6 | 1.8 | 25.0 | 51.2 | 220.7 | 70.9 | 362.7 | 48.6 | 4.8 | 0.3 | 8.4 | 0.6 | 390.3 | 2.0 |
| ZK-18-08B | 82.1 | 319.0 | 40.5 | 1.9 | 25.5 | 47.7 | 219.8 | 68.1 | 375.4 | 48.9 | 4.6 | 0.4 | 8.8 | 0.6 | 428.5 | 2.1 |
| ZK-18-09 | 39.5 | 214.9 | 39.6 | 1.9 | 25.1 | 56.3 | 238.1 | 75.7 | 369.5 | 52.2 | 3.6 | 0.2 | 8.7 | 0.6 | 230.1 | 1.9 |
| ZK-18-10 | 47.8 | 390.7 | 34.6 | 1.7 | 24.9 | 51.5 | 224.7 | 70.9 | 352.9 | 48.8 | 2.6 | 0.3 | 8.3 | 0.6 | 346.8 | 2.1 |
| ZK-18-11 | 35.2 | 154.1 | 39.7 | 2.0 | 24.9 | 58.2 | 240.0 | 76.4 | 340.1 | 52.5 | 3.6 | 0.2 | 8.8 | 0.6 | 191.1 | 1.9 |
| ZK-18-12 | 53.7 | 108.2 | 36.5 | 1.8 | 22.4 | 51.3 | 222.0 | 69.6 | 329.6 | 45.1 | 3.2 | 0.3 | 8.5 | 0.6 | 297.5 | 1.7 |
| **Average** | 42.9 | 212.7 | 39.3 | 1.9 | 25.4 | 54.8 | 238.0 | 73.5 | 366.3 | 51.5 | 2.7 | 0.3 | 8.8 | 0.6 | 250.3 | 2.0 |
| **Std** | 21.9 | 90.2 | 2.6 | 0.1 | 1.6 | 5.4 | 18.9 | 4.9 | 17.2 | 4.1 | 1.3 | 0.1 | 0.6 | 0.0 | 94.7 | 0.1 |
| **Min** | 16.7 | 108.2 | 34.6 | 1.7 | 22.4 | 46.7 | 219.1 | 66.6 | 329.6 | 45.1 | 1.1 | 0.2 | 8.3 | 0.5 | 136.6 | 1.7 |
| **Max** | 82.1 | 390.7 | 46.1 | 2.2 | 29.7 | 64.8 | 279.8 | 83.6 | 392.3 | 61.1 | 4.8 | 0.4 | 10.2 | 0.7 | 428.5 | 2.2 |

0

1

2

**Table -3** :- REE data of Panjal Traps from Zanskar region

| Sample ID | La | Ce | Pr | Nd | Sm | Eu | Gd | Tb | Dy | Ho | Er | Tm | Yb | Lu | Eu/Eu* |
|---|---|---|---|---|---|---|---|---|---|---|---|---|---|---|---|
| | | | | | | | | µg/g | | | | | | | |
| ZK-18-01 | 10.0 | 24.6 | 3.5 | 15.5 | 4.3 | 1.3 | 4.7 | 0.8 | 4.8 | 0.9 | 2.5 | 0.33 | 1.8 | 0.2 | 0.87 |
| ZK-18-02 | 16.0 | 36.8 | 4.9 | 20.7 | 5.2 | 1.6 | 5.7 | 1.0 | 5.6 | 1.1 | 2.8 | 0.37 | 2.1 | 0.3 | 0.89 |
| ZK-18-03 | 9.6 | 23.7 | 3.3 | 15.0 | 4.2 | 1.3 | 4.7 | 0.8 | 5.0 | 1.0 | 2.5 | 0.33 | 1.9 | 0.2 | 0.88 |
| ZK-18-04A | 9.0 | 22.4 | 3.2 | 14.2 | 4.0 | 1.3 | 4.5 | 0.8 | 4.8 | 0.9 | 2.4 | 0.33 | 1.9 | 0.2 | 0.91 |
| ZK-18-04B | 9.7 | 23.5 | 3.4 | 15.0 | 4.2 | 1.3 | 4.7 | 0.8 | 5.0 | 1.0 | 2.5 | 0.33 | 1.9 | 0.2 | 0.87 |
| ZK-18-05 | 11.9 | 27.7 | 3.6 | 15.7 | 4.2 | 1.5 | 4.5 | 0.8 | 4.6 | 0.9 | 2.4 | 0.34 | 2.0 | 0.3 | 0.01 |
| ZK-18-06 | 12.0 | 27.3 | 3.6 | 15.3 | 4.1 | 1.4 | 4.4 | 0.8 | 4.5 | 0.9 | 2.4 | 0.33 | 1.9 | 0.3 | 1.00 |
| ZK-18-07 | 12.3 | 27.0 | 3.6 | 15.2 | 4.1 | 1.4 | 4.4 | 0.7 | 4.4 | 0.9 | 2.3 | 0.33 | 1.9 | 0.3 | 0.99 |
| ZK-18-08A | 11.8 | 27.0 | 3.6 | 15.5 | 4.2 | 1.5 | 4.5 | 0.8 | 4.6 | 0.9 | 2.4 | 0.34 | 1.9 | 0.3 | 1.04 |
| ZK-18-08B | 12.3 | 28.3 | 3.7 | 16.1 | 4.2 | 1.5 | 4.6 | 0.8 | 4.7 | 0.9 | 2.4 | 0.34 | 2.0 | 0.3 | 1.00 |
| ZK-18-09 | 12.7 | 28.4 | 3.7 | 16.3 | 4.1 | 1.5 | 4.5 | 0.8 | 4.7 | 0.9 | 2.4 | 0.32 | 1.9 | 0.2 | 1.04 |
| ZK-18-10 | 11.1 | 26.3 | 3.5 | 14.9 | 3.9 | 1.3 | 4.3 | 0.8 | 4.5 | 0.9 | 2.4 | 0.33 | 1.9 | 0.3 | 0.99 |
| ZK-18-11 | 9.5 | 23.9 | 3.4 | 15.3 | 4.2 | 1.3 | 4.5 | 0.8 | 4.6 | 0.9 | 2.3 | 0.32 | 1.9 | 0.2 | 0.91 |
| ZK-18-12 | 10.4 | 26.1 | 3.5 | 15.5 | 4.0 | 1.2 | 4.5 | 0.7 | 4.4 | 0.9 | 2.2 | 0.29 | 1.7 | 0.2 | 0.87 |
| **Average** | 11.3 | 26.6 | 3.6 | 15.7 | 4.2 | 1.4 | 4.6 | 0.8 | 4.7 | 0.9 | 2.4 | 0.3 | 1.9 | 0.2 | 0.9 |
| **Std** | 1.8 | 3.5 | 0.4 | 1.5 | 0.3 | 0.1 | 0.3 | 0.1 | 0.3 | 0.1 | 0.1 | 0.0 | 0.1 | 0.0 | 0.3 |
| **Min** | 9.0 | 22.4 | 3.2 | 14.2 | 3.9 | 1.2 | 4.3 | 0.7 | 4.4 | 0.9 | 2.2 | 0.3 | 1.7 | 0.2 | 0.0 |
| **Max** | 16.0 | 36.8 | 4.9 | 20.7 | 5.2 | 1.6 | 5.7 | 1.0 | 5.6 | 1.1 | 2.8 | 0.4 | 2.1 | 0.3 | 1.0 |

3

# 6.Discussion

## 6.1. Classification

The total alkali versus silica (TAS) diagram is one of the widely used methods for classifying igneous rocks (Le Bas et al., 1986). This diagram provides a complete outline for understanding the composition and characteristics of igneous rocks based on their silica content and total alkali content ($Na_2O$ and $K_2O$). The field boundaries shown in the diagram outline distinct regions corresponding to different types of igneous rocks, further classification into ultrabasic, basic, intermediate, and acidic categories, further enhances the utility of the TAS diagram. In the context of the Zanskar region, the application of the TAS diagram reveals the presence of basic igneous rock types (Figure 4). The collected samples from Zanskar fall within the fields of Basalts, trachy-basalt, and basaltic andesite. The basalts, basaltic trachyandesites, and trachybasalt can be classified as sub-alkaline basalt (Winchester and Floyd, 1977; Figure 5a). All the samples are mostly metaluminous and falling in range of high-K calc-alkaline rocks (Figure 5b) Peccerillo and Taylor 1976). The $SiO_2$ vs $K_2O$ plot classifies the samples as calc-alkaline basalts to high K-calc alkaline basalts, further substantiating their sub-alkaline classification (Figure 5b; Peccerillo and Taylor, 1976). The AFM diagram proposed by Irvine and Baragar (1971) also provide evidence for this classification (Figure 5c). The $Al_2O_3$ vs Alkali plot derived by Shands (1943) confirms the metaaluminous confirmation for these basalts. (Figure 5d)

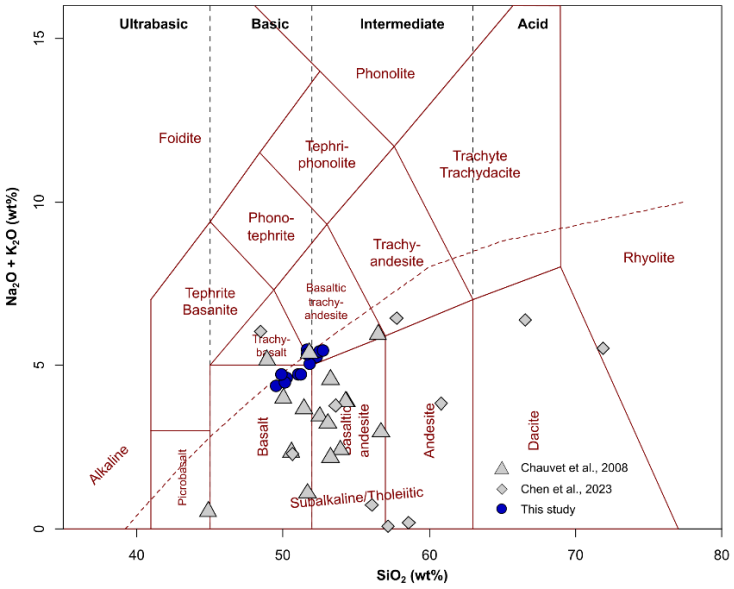


**Figure. 4:** Total Alkali Silica (TAS) classification diagram showing the different rock types from Zanskar region (Le Bas et al., 1986).

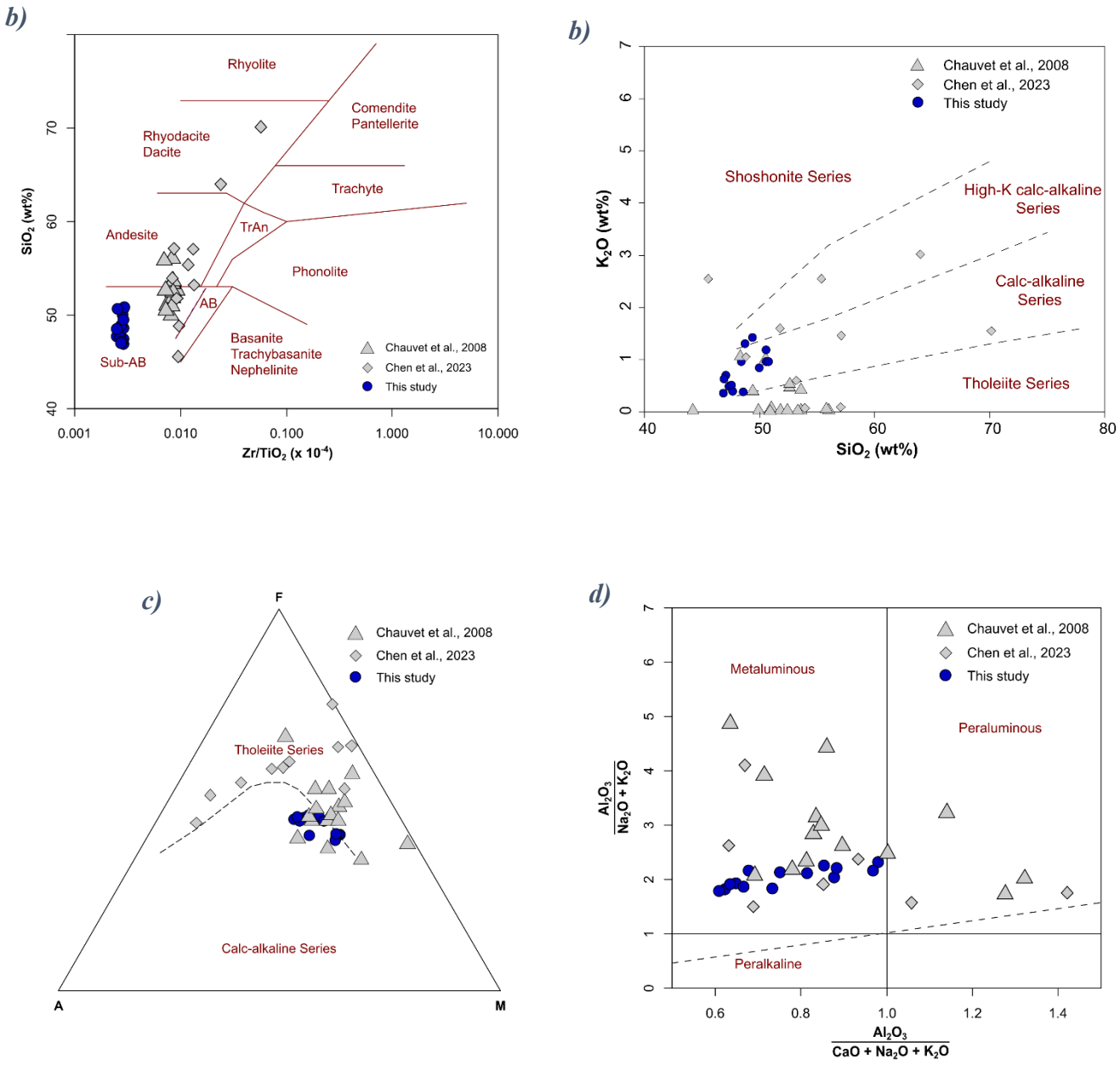


**Figure 5.** (a) $SiO_2$ vs $Zr/TiO_2$ Plot by Winchester and Floyd (1977) (b) $SiO_2$ vs $K_2O$ Plot by Peccerillo and Taylor (1976) (c) AFM Plot by Irvine and Baragar (1971) (d) $Al_2O_3$ vs Alkali Plot by Shands (1943)

## 6.2. Crustal contamination and assimilation

Continental flood basalts from LIPs frequently display effects of crustal assimilation (e.g. Sheth et al., 2013). The trace elemental ratios such as Nb/U, Nb/La, $Th/Nb_{PM}$, and Th/Ta, serve as proxies for understanding crustal assimilation effects since they remain unaltered by fractional crystallization and/or partial melting. MORB (E-MORB and N-MORB) and Primitive mantle are chemically characterized by high Nb/U (>30), Nb/La (>0.9), Th/Ta (>2.1)

and $Th/Nb_{PM}$ (≤1) ratios (Campbell, 2002; Saunders et al., 1992). Incompatible elements such as Th are usually more concentrated in the crust, while less incompatible elements (i.e. Nb and Ta) show depletion (Campbell, 2002; Rudnick and Gao, 2003). The average Nb/U value of Nb/La value of ~0.5, Upper Crust is ~0.5, Th/Ta value of >10, and $(Th/Nb)_{PM}$ value of more than (>7; Campbell, 2002; Saunders et al., 1992).Uncontaminated basalts generally show higher Nb/U, Nb/La, and lower Th/Yb values compared to the contaminated basalts. Therefore, these trace element ratios can act as indicators for crustal assimilation for basaltic rocks.

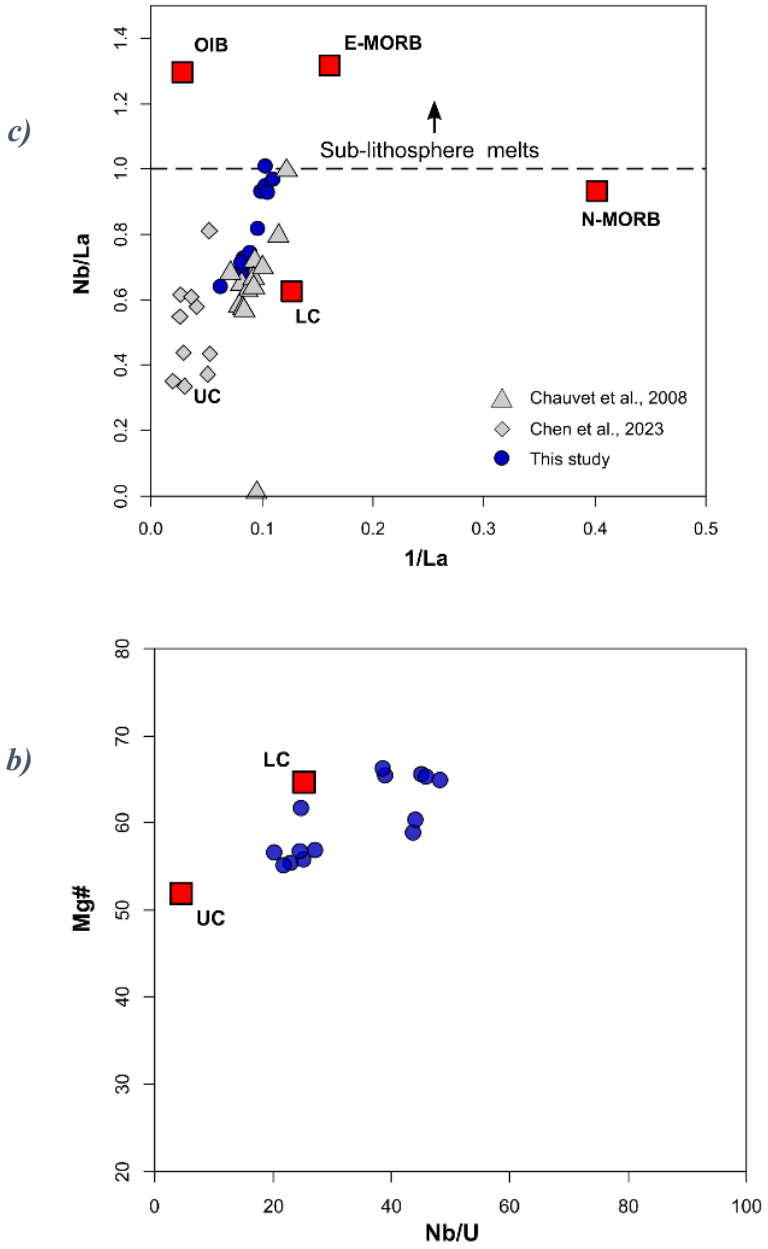


**Figure 6.** a) Nb/La vs. 1/La plot for the Panjal Traps of Zanskar Region. This plot depicts source magma affinity towards a crustal source b) Mg# vs Nb/U plot for Zanskar samples.

The Nb/La values of most of the Zanskar samples are close to 1.0 (average ~0.8). The Nb/U values can be used to separate the samples into basalts (ZK-18-01, 02, 03, 04) which is ~43 and basaltic trachyandesite (ZK-18-05, 07, 08) samples show set of lower values ~28. (Figure 6a). The other trace element discrimination diagrams also show separate clusters for basalt samples (ZK-18-01, 02, 03, 04) and basaltic trachyandesite (ZK-18-05, 07, 08) (Figure 6b). Similarly, a cross-plot between $TiO_2$ and $(Th/Nb)_{PM}$ shows that the Zanskar samples fall in the theoretical limit of 0-5% partial assimilation of the average upper crust (Figure 7). This evidence suggest that samples have limited crustal contamination.

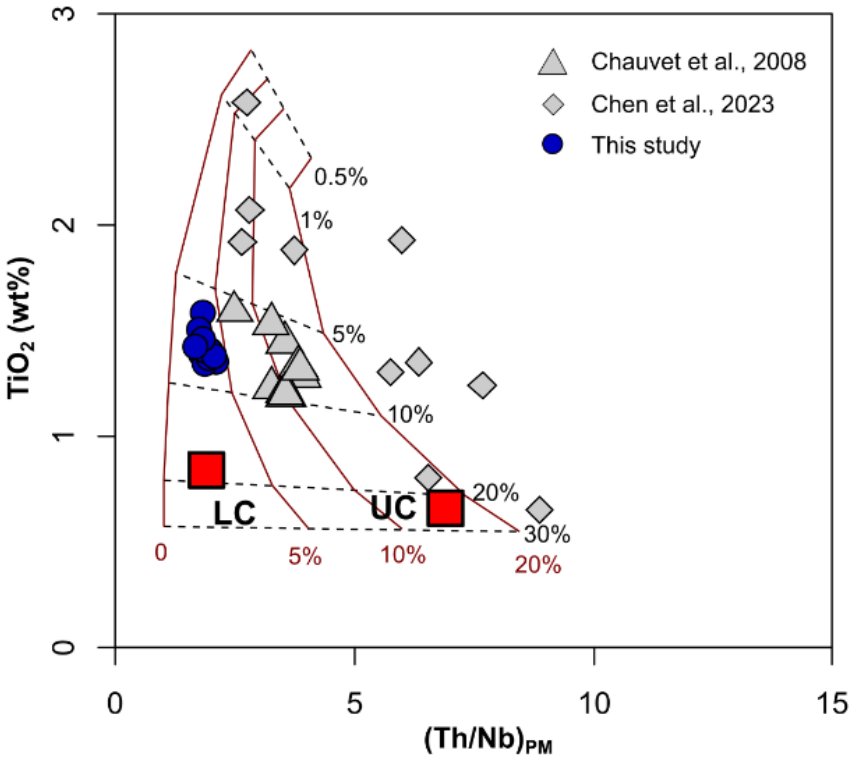


**Figure 7**. $TiO_2$ (wt.%) vs. $Th/Nb_{PM}$ showing partial melting of spinel peridotite source (vertical) with assimilation of crustal melts silicic Panjal Traps; Shellnut., 2017). The solid sub-horizontal represents amount of partial melting (i.e. 0.5%, 1%, 5%, 10%, 20% and 30%).

## 6.3. Petrogenesis and Fractional crystallization

Trace element ratios can indicate whether magmatic processes in the mantle are open (assimilation) or closed (fractional crystallization) (Baksi, 2001; Condie, 2003). Because of high HREE and Y distribution coefficients in garnet, the Zr/Y and Nb/Y ratios in mafic rocks change based on the degree of partial melting (of the mantle) and the depth of melting (Baksi, 2001; Class et al., 1998). The degree to which of partial melting of the source occurred is critical since large degrees of partial melting consume garnet from the source, resulting in low trace element ratios (La/Yb, Zr/Y). The low Nb/Y and Zr/Y ratios of the Zanskar samples suggest that the source of the melt was shallow (Baksi, 2001), compared to the Normal Mid-Ocean Ridge Basalts (N-MORB), Enriched Mid-Ocean Ridge Basalts (E-MORB), Primitive Mantle (PM), and Ocean Island Basalts (OIB) (Sun and McDonough, 1989).

The chondrite-normalized REE plots of samples from Zanskar exhibit similar trends to those observed in previous studies (Chauvet et al., 2008). The relatively flat HREE patterns and low $(La/Yb)_N$ ratios (3.5 to 5.29) indicate that the basalts did not originate from a garnet-bearing peridotite source. The samples correlate perfectly with the REE trends observed by (Chauvet et al., 2009). In a cross plot between $TiO_2$ and $(Th/Nb)_{PM}$ the Zanskar samples falls within the theoretical range of moderate degrees (5-10%) of partial melting of a spinel peridotite source (Figure 7).

The Pearce element ratios (PERs) are widely used to determine the existence of fractional crystallization from a parent magma (Pearce et al., 1968). This ratio is calculated using the proportions of major elements in the minerals of basaltic minerals (olivine, plagioclase, and pyroxene) in relation one that is unaffected by fractionation (conserved element such as Ti). PERs have the advantage over the generally used Harker diagram as it minimizes the impact of constant sum problem. In the Pearce diagram (Figure 8a), the samples show a high slope (>2), trending similar to olivine-controlled fractionation pattern. A similar observation can be observed from the MgO vs CaO (Figure 8b) plot in which also shows a trend parallel to the olivine fractionation line. This suggests early olivine fractionation of the parental magma source.

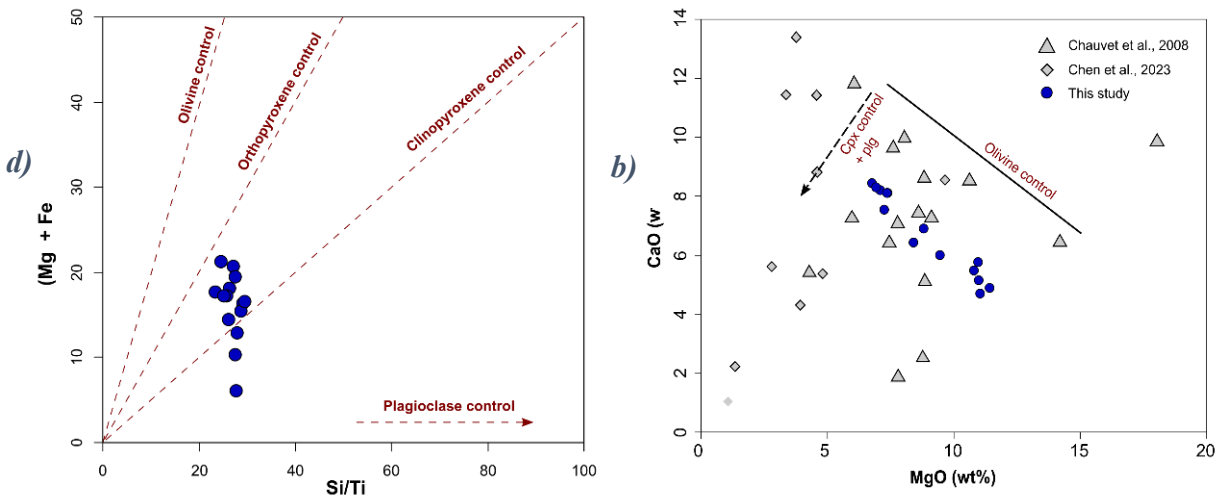


**Figure 8.** (a) Si/Ti vs (Mg+Fe)/Ti (PER) plot by (Pearce, 1968; Russell and Nicholls, (1988,1990) b) MgO (wt%) vs CaO plot of Panjal Traps

## 6.4. Tectono-magmatic evolution and regional implications

Mantle plumes are believed to play a significant role in the creation of numerous LIPs (Campbell, 2007; Bryan and Ernst, 2008). The close connection between LIPs and volcanic rifted margins signifies the role of mantle plumes in facilitating continental breakup (Courtillot et al., 1999). Tomographic images of oceanic crust beneath hotspots support this proposition. It appears that while the mantle plume model applies to some LIPs, it is not universally applicable (McHone, 2000; Sheth, 2005, 2007a), b). Passive rifting and thermal convection models are also used to explain the origins of LIPs (Anderson, 2005; Foulger et al., 2005).

Existing studies have proposed that the progression of sedimentation pattern from marine to continental modes in the Kashmir and Zanskar valleys display evidence of crustal uplift before and during the eruption of the Panjal Traps. This is process is attributed to crustal rifting and thinning in contrast to plume-induced doming (Gaetani et al., 1990; Srikantia and Bhargava, 1983). Basalt compositions at Guryal Ravine, Pahalgam, and Zanskar-Spiti resemble contaminated Enriched Mid-Ocean Ridge Basalts (E-MORB) (Figure 9a) in contrast to flood basalts from other LIPs, which exhibit OIB characteristics (Shellnut et al., 2014). For the Zanskar samples, low Nb/Y, $(La/Yb)_N$, and Zr/Y ratios suggest a shallow spinel-peridotite source. Consistent with other studies, the geochemical characteristics of the Panjal Traps from the Zanskar region align well with basalts associated with plate separation and ocean basin formation from the Central Atlantic Magmatic Province. This chemistry is different from

basalts of the Tarim LIP and the Emeishan Large Igneous Province (ELIP), where plate separation mechanisms are not observed (Shellnut et al., 2014). Although a mantle-plume origin is generally considered for the and Tarim and ELIP basalts, there exists no consensus on the role of mantle plume activity in the generation of the Panjal Traps (McHone, 2000; Xiao et al., 2004; Murphy et al., 2011; Xu et al., 2011). Hence, prevailing evidences suggest that a deep mantle-plume origin for the Panjal Traps seems unlikely.

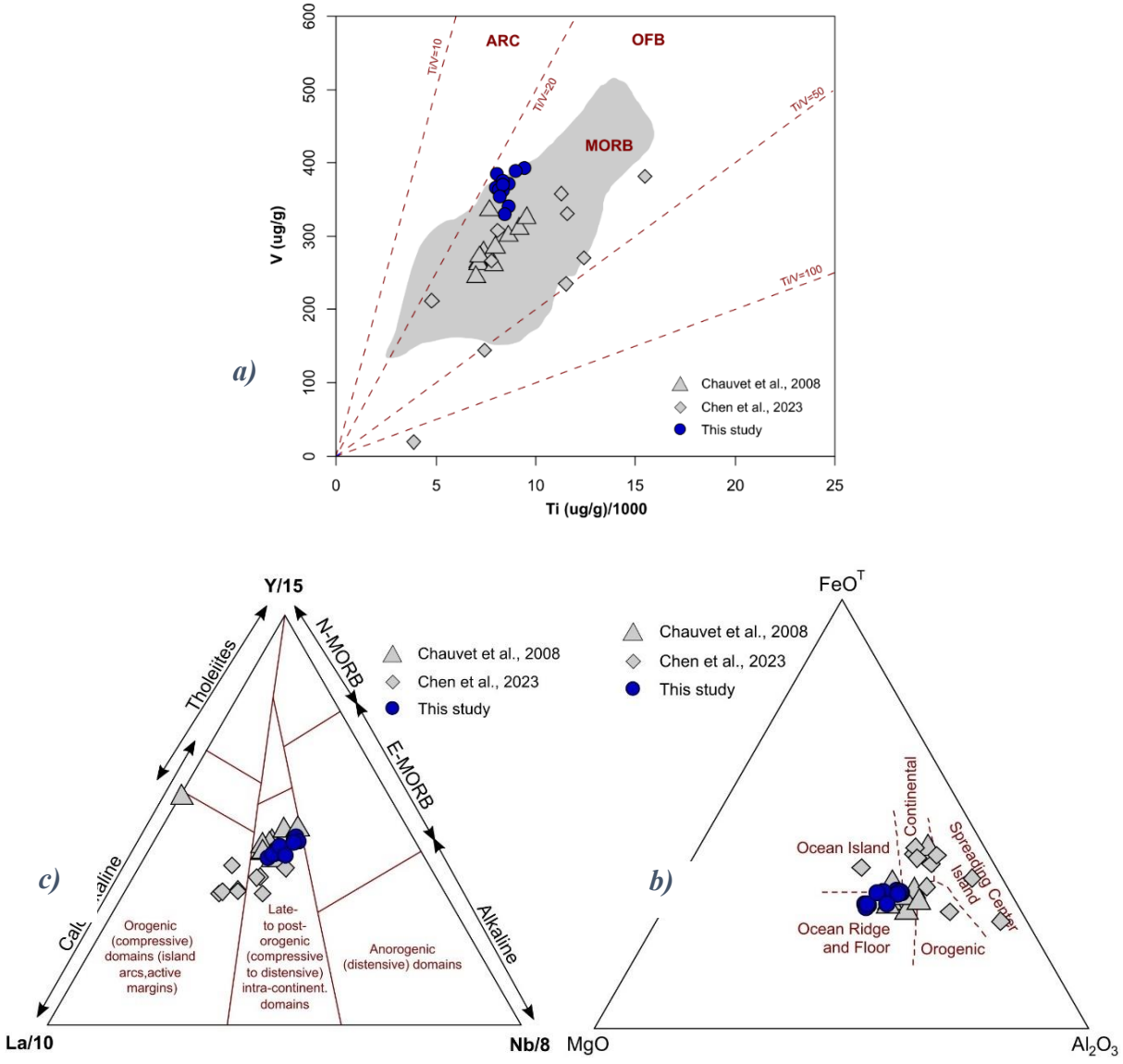


**Figure 9.** (a) Basalt tectonomagmatic discrimination diagrams for the mafic Panjal Traps (a) Shervais (1982) (b) Pearce et al. (1977) (c) Cabanis and Lecolle (1989)

On a regional scale, the Panjal Traps share contemporaneity with numerous magmatic rocks associated with the rifting of Cimmerian microcontinental blocks. These include the Abor volcanics, and associated granitic plutons and volcanic rocks (Ali et al., 2012; Bhat, 1984;

Sengor, 1984; Spring et al., 1993). A correlation between the Panjal Traps and the middle Permian Jilong and Selong basalts in Tibet was proposed by Zhu et al. (2010), suggesting their potential as their easternmost extension. However, no consensus exists till date since in both temporal and geochemical characteristics argue against a direct relationship. Temporallu, the Panjal Traps are dated older (~290 Myr) than the Jilong and Selong basalts (<280 Myr; Shellnutt et al., 2011; Zhu et al., 2010). Geochemically, the Panjal Traps exhibit greater range of $TiO_2$ values (< 3.2), lower MgO (<10wt%), lower Mg# (rarely exceeding 65), and lower Ni content (<200 μg/g). In contrast, moderate $TiO_2$ (1.8 to 2.0 wt.%), high MgO (>12 wt.%), high Mg# (>65), and high Ni (>200 μg/g) are generally observed for the Jilong and Selong basalts. In summary, while being distinct magmatic systems and indirectly related, both the Jilong and Selong basalts and the Himalayan Panjal Traps, represent the same regional-scale rifting of the northern Gondwana margin. Such a similar relationship may also be likely applicable to the Abor volcanic rocks (Ali et al., 2012; Bhat, 1984).

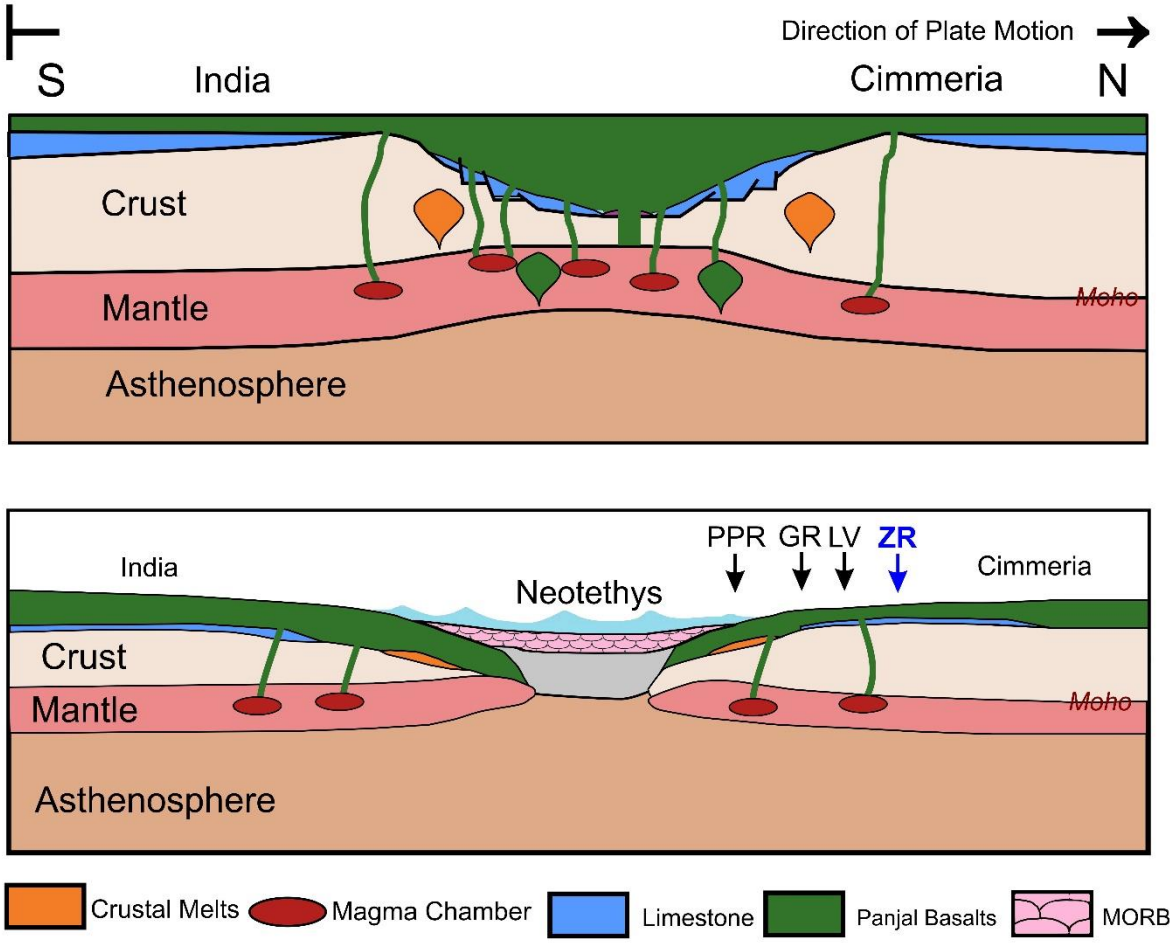


**Figure 10**. Model depicting the tectonic evolution for the southern Paleotethys opening during the eruption of Panjal Traps (modified from Shellnut, 2016).The different exposures of Panjal volcanism are indicated (Pir Panjal Range (PPR), Guryal Ravine (GR), and Lidder Valley (LV) Zanskar Valley (ZR)).

# Conclusions

This study focuses on the geochemical characterization of the Panjal Traps, from the Zanskar region, North western Himalayas. The samples from Zanskar can be classified into basalts, basaltic trachyandesites, and trachyandesites, all predominantly exhibiting a calc-alkaline nature with notably high MgO content (wt%). Geochemical analysis reveal enriched LREE and flat HREE trends. High Nb/U (>30), Nb/La (>0.9), and $Th/Nb_{PM}$ ($\leq$1) ratios, suggest that the magma was generated by partial melting (~5%-10%) of a spinel peridotite source at shallow depths (<75 km). Trends observed in Pearce Elemental Ratios indicate an early olivine-controlled fractionation of this parental magma. Further, $Th/Nb_{PM}$ vs $TiO_2$ ratios suggest minimal (~5%) crustal assimilation. Analysis of tectono-magmatic diagrams suggests that the eruption occurred in an oceanic ridge setting, with basalts exhibiting characteristics of E-MORB in a passive margin setup. These observations align well with previously reported data on the Panjal Traps in the Kashmir Valley (Chen et al., 2023), although they show lateral variability in composition compared to the Panjal Traps from Lahul-Spiti (Chauvet et al., 2008).

# References


Ali, S.A., Buckman, S., Aswad, K.J., Jones, B.G., Ismail, S.A. and Nutman, A.P., 2012. Recognition of Late Cretaceous Hasanbag ophiolite-arc rocks in the Kurdistan Region of the Iraqi Zagros suture zone: A missing link in the paleogeography of the closing Neotethys Ocean. Lithosphere, 4(5), pp.395-410.

Anderson, J., Bachu, S., Nimir, H.B., Basu, B., Bradshaw, J., Deguchi, G., Gale, J., von Goerne, G., Heidug, W., Holloway, S. and Kamal, R., 2005. Underground geological storage. Cambridge University Press.

Baksi, A.K., 2001. Search for a deep-mantle component in mafic lavas using a Nb Y Zr plot. Canadian Journal of Earth Sciences, 38(5), pp.813-824.

Bas, M.L., Maitre, R.L., Streckeisen, A., Zanettin, B. and IUGS Subcommission on the Systematics of Igneous Rocks, 1986. A chemical classification of volcanic rocks based on the total alkali-silica diagram. Journal of petrology, 27(3), pp.745-750.

Bhat, M.I., Zainuddin, S.M. and Rais, A., 1981. Panjal Trap chemistry and the birth of Tethys. Geological Magazine, 118(4), pp.367-375.

Brookfield, M.E., Stebbins, A.G., Williams, J.C., Wolbach, W.S., Hannigan, R. and Bhat, G.M., 2020. Palaeoenvironments and elemental geochemistry across the marine Permo-Triassic boundary section, Guryul Ravine (Kashmir, India) and a comparison with other North Indian passive margin sections. The Depositional Record, 6(1), pp.75-116.

Bryan, S.E. and Ernst, R.E., 2008. Revised definition of large igneous provinces (LIPs). Earth-Science Reviews, 86(1-4), pp.175-202.



Bryan, S.E. and Ernst, R.E., 2008. Revised definition of large igneous provinces (LIPs). Earth-Science Reviews, 86(1-4), pp.175-202.



Campbell, I.H., 2007. Testing the plume theory. Chemical Geology, 241(3-4), pp.153-176.

Chauvet, F., Lapierre, H., Bosch, D., Guillot, S., Mascle, G., Vannay, J.C., Cotten, J., Brunet, P. and Keller, F., 2008. Geochemistry of the Panjal Traps basalts (NW Himalaya): records of the Pangea Permian break-up. Bulletin de la Société géologique de France, 179(4), pp.383-395.

Chen, W.Y., Shellnutt, J.G., Bhat, G.M., Tejada, M.L.G., Suzuki, K. and Denyszyn, S.W., 2023. Geochronology and geochemistry of the Panjal Traps from the southern Pir Panjal Range, Kashmir, India. Lithos, 436, p.106967.

Condie, K.C., 2003. Supercontinents, superplumes and continental growth: the Neoproterozoic record. Geological Society, London, Special Publications, 206(1), pp.1-21.

Dercourt, J., Ricou, L.E. and Vrielynck, B., 1993. Atlas Tethys Palaeoenvironmental Maps Gauthier-Villars. Paris 307pp, 14.

Ernst, R.E., 2014. Large igneous provinces. Cambridge University Press.

Foulger, G.R., Natland, J.H., Presnall, D.C. and Anderson, D.L., 2005. Plates, plumes and paradigms. Geological Society of America.

Foulger, G.R., Natland, J.H., Presnall, D.C. and Anderson, D.L., 2005. Plates, plumes and paradigms. Geological Society of America.

Fuchs, G.E.R.H.A.R.D., 1987. The geology of southern Zanskar (Ladakh)-Evidence for the autochthony of the Tethys zone of the Himalaya. Jahrbuch der Geologischen Bundesanstalt, 130(4), pp.465-491.

Gaetani, M., Gosso, G. and Pognante, U., 1990. A geological transect from Kun Lun to Karakorum (Sinkiang, China): the western termination of the Tibetan Plateau. Preliminary note. Terra nova, 2(1), pp.23-30.

Gao, S., Rudnick, R.L., Yuan, H.L., Liu, X.M., Liu, Y.S., Xu, W.L., Ling, W.L., Ayers, J., Wang, X.C. and Wang, Q.H., 2004. Recycling lower continental crust in the North China craton. Nature, 432(7019), pp.892-897.

Garzanti, E., Le Fort, P. and Sciunnach, D., 1999. First report of Lower Permian basalts in South Tibet: tholeiitic magmatism during break-up and incipient opening of Neotethys. Journal of Asian Earth Sciences, 17(4), pp.533-546.

Garzanti, E., Nicora, A. and Rettori, R., 1998. Permo-Triassic boundary and lower to middle Triassic in South Tibet. Journal of Asian Earth Sciences, 16(2-3), pp.143-157.

Honegger, K., Dietrich, V., Frank, W., Gansser, A., Thöni, M. and Trommsdorff, V., 1982. Magmatism and metamorphism in the Ladakh Himalayas (the Indus-Tsangpo suture zone). Earth and Planetary Science Letters, 60(2), pp.253-292.

Irvine, T.N. and Baragar, W.R.A.F., 1971. A guide to the chemical classification of the common volcanic rocks. Canadian journal of earth sciences, 8(5), pp.523-548.

Kapoor, H.M., 1977. Pastannah section of Kashmir with special reference to ‘ Ophioceras’bed of Middlemiss. J. Palaeontol. Soc. India, 20, pp.339-347.

López-Maury, L., Marguerat, S. and Bähler, J., 2008. Tuning gene expression to changing environments: from rapid responses to evolutionary adaptation. Nature Reviews Genetics, 9(8), pp.583-593.

McHone, J.G., 2000. Non-plume magmatism and rifting during the opening of the central Atlantic Ocean. Tectonophysics, 316(3-4), pp.287-296.

Middlemiss, C.S., 1910. ... The Kangra Earthquake of 4th April 1905 (Vol. 38). Geological survey of India.

Murphy, J.B., Dostal, J., Gutiérrez-Alonso, G. and Keppie, J.D., 2011. Early Jurassic magmatism on the northern margin of CAMP: Derivation from a Proterozoic sub-continental lithospheric mantle. Lithos, 123(1-4), pp.158-164.

Nakazawa, K., Kapoor, H.M., Ishii, K.I., Bando, Y., Okimura, Y. and Tokuoka, T., 1975. The upper Permian and the lower Triassic in Kashmir, India. Memoirs of the Faculty of Science, Kyoto University. Series of geology and mineralogy, 42(1), pp.1-106.

Oldow, J.S., Ferranti, L., Lewis, D.S., Campbell, J.K., d'Argenio, B., Catalano, R., Pappone, G., Carmignani, L., Conti, P. and Aiken, C.L.V., 2002. Active fragmentation of Adria, the north African promontory, central Mediterranean orogen. Geology, 30(9), pp.779-782.

Pareek, H.S., 1988. Petrographic characteristics of the solid fuels of India with particular reference to the coking coals. International journal of coal geology, 10(3), pp.285-306.

Pearce, T.H., 1968. A contribution to the theory of variation diagrams. Contributions to Mineralogy and Petrology, 19(2), pp.142-157.

Peccerillo, A. and Taylor, S.R., 1976. Geochemistry of Eocene calc-alkaline volcanic rocks from the Kastamonu area, northern Turkey. Contributions to mineralogy and petrology, 58, pp.63-81.

Rameshwar Rao, D. and Rai, H., 2007. Permian komatiites and associated basalts from the marine sediments of Chhongtash Formation, southeast Karakoram, Ladakh, India. Mineralogy and Petrology, 91, pp.171-189.

Rampino, M.R. and Stothers, R.B., 1988. Flood basalt volcanism during the past 250 million years. Science, 241(4866), pp.663-668.

Reichow, M.K., Pringle, M.S., Al'Mukhamedov, A.I., Allen, M.B., Andreichev, V.L., Buslov, M.M., Davies, C.E., Fedoseev, G.S., Fitton, J.G., Inger, S. and Medvedev, A.Y., 2009. The timing and extent of the eruption of the Siberian Traps large igneous province: Implications for the end-Permian environmental crisis. Earth and Planetary Science Letters, 277(1-2), pp.9-20.

Richards, M.A., Duncan, R.A. and Courtillot, V.E., 1989. Flood basalts and hot-spot tracks: plume heads and tails. Science, 246(4926), pp.103-107.

Rousseau, D.D., Puisségur, J.J. and Lécolle, F., 1992. West-European terrestrial molluscs assemblages of isotopic stage 11 (Middle Pleistocene): climatic implications. Palaeogeography, Palaeoclimatology, Palaeoecology, 92(1-2), pp.15-29.

Russell, J.K. and Nicholls, J., 1988. Analysis of petrologic hypotheses with Pearce element ratios. Contributions to Mineralogy and Petrology, 99(1), pp.25-35.

Samanta, A., Tripathy, G.R., Nath, B.N., Bhushan, R., Panchang, R., Bharti, N. and Shrivastava, A., 2022. Holocene variability in chemical weathering and ocean redox state: A reconstruction using sediment geochemistry of the Arabian Sea. Journal of Asian Earth Sciences, 224, p.105029.

Saunders, A.D., Storey, M., Kent, R.W. and Norry, M.J., 1992. Consequences of plume-lithosphere interactions. Geological Society, London, Special Publications, 68(1), pp.41-60.

Şengör, A.M.C., 1987. Cross-faults and differential stretching of hanging walls in regions of low-angle normal faulting: examples from western Turkey. Geological Society, London, Special Publications, 28(1), pp.575-589.

Şengör, A.M.C., Yılmaz, Y. and Sungurlu, O., 1984. Tectonics of the Mediterranean Cimmerides: nature and evolution of the western termination of Palaeo-Tethys. Geological Society, London, Special Publications, 17(1), pp.77-112.

Shand, S.J., 1942. Phase petrology in the Cortlandt complex, New York. Bulletin of the Geological Society of America, 53(3), pp.409-428.

Shellnutt, J.G. and Zhou, M.F., 2007. Permian peralkaline, peraluminous and metaluminous A-type granites in the Panxi district, SW China: their relationship to the Emeishan mantle plume. Chemical Geology, 243(3-4), pp.286-316.

Shellnutt, J.G., 2018. The panjal traps.

Shellnutt, J.G., Bhat, G.M., Brookfield, M.E. and Jahn, B.M., 2011. No link between the Panjal Traps (Kashmir) and the Late Permian mass extinctions. Geophysical Research Letters, 38(19).

Shellnutt, J.G., Bhat, G.M., Wang, K.L., Brookfield, M.E., Jahn, B.M. and Dostal, J., 2014. Petrogenesis of the flood basalts from the Early Permian Panjal Traps, Kashmir, India: Geochemical evidence for shallow melting of the mantle. Lithos, 204, pp.159-171.

Shellnutt, J.G., Bhat, G.M., Wang, K.L., Yeh, M.W., Brookfield, M.E. and Jahn, B.M., 2015. Multiple mantle sources of the early Permian Panjal traps, Kashmir, India. American Journal of Science, 315(7), pp.589-619.

Shellnutt, J.G., Lee, T.Y., Brookfield, M.E. and Chung, S.L., 2014. Correlation between magmatism of the Ladakh Batholith and plate convergence rates during the India–Eurasia collision. Gondwana Research, 26(3-4), pp.1051-1059.

Shervais, J.W., Vetter, S.K. and Hanan, B.B., 2006. Layered mafic sill complex beneath the eastern Snake River Plain: Evidence from cyclic geochemical variations in basalt. Geology, 34(5), pp.365-368.

Sheth, H.C., Zellmer, G.F., Kshirsagar, P.V. and Cucciniello, C., 2013. Geochemistry of the Palitana flood basalt sequence and the Eastern Saurashtra dykes, Deccan Traps: clues to petrogenesis, dyke–flow relationships, and regional lava stratigraphy. Bulletin of Volcanology, 75, pp.1-23.

Srikantia, S.V., 1987. Himalaya—the collided orogen: a plate tectonic evolution on geological evidences. Tectonophysics, 134(1-3), pp.75-90.

Stampfli, G., Marcoux, J. and Baud, A., 1991. Tethyan margins in space and time. Palaeogeography, Palaeoclimatology, Palaeoecology, 87(1-4), pp.373-409.

Stojanovic, D., Aitchison, J.C., Ali, J.R., Ahmad, T. and Dar, R.A., 2016. Paleomagnetic investigation of the Early Permian Panjal Traps of NW India; regional tectonic implications. Journal of Asian Earth Sciences, 115, pp.114-123.

Sun, S.S. and McDonough, W.F., 1989. Chemical and isotopic systematics of oceanic basalts: implications for mantle composition and processes. Geological Society, London, Special Publications, 42(1), pp.313-345.

Timmerman, M.J., Heeremans, M., Kirstein, L.A., Larsen, B.T., Spencer-Dunworth, E.A. and Sundvoll, B., 2009. Linking changes in tectonic style with magmatism in northern Europe during the late Carboniferous to latest Permian. Tectonophysics, 473(3-4), pp.375-390.

van de Schootbrugge, B.A.S. and Wignall, P.B., 2016. A tale of two extinctions: converging end-Permian and end-Triassic scenarios. Geological Magazine, 153(2), pp.332-354.

Vannay, J.C. and Spring, L., 1993. Geochemistry of the continental basalts within the Tethyan Himalaya of Lahul-Spiti and SE Zanskar, northwest India. Geological Society, London, Special Publications, 74(1), pp.237-249.

Veevers, J.J. and Tewari, R.C., 1995. Permian-Carboniferous and Permian-Triassic magmatism in the rift zone bordering the Tethyan margin of southern Pangea. Geology, 23(5), pp.467-470.

Wadia, D.N., 1934. The Cambrian-Trias sequence of North-West Kashmir (parts of Muzafarabad and Baramula Districts). Records of Geological Survey of India, 68, p.121.

White, L.T., Gibson, G.M. and Lister, G.S., 2013. A reassessment of paleogeographic reconstructions of eastern Gondwana: Bringing geology back into the equation. Gondwana Research, 24(3-4), pp.984-998.

White, R.V. and Saunders, A.D., 2005. Volcanism, impact and mass extinctions: incredible or credible coincidences?. Lithos, 79(3-4), pp.299-316.

Wignall, P.B., 2001. Large igneous provinces and mass extinctions. Earth-science reviews, 53(1-2), pp.1-33.

Winchester, J.A. and Floyd, P.A., 1977. Geochemical discrimination of different magma series and their differentiation products using immobile elements. Chemical geology, 20, pp.325-343.

Yang, T.N., Ding, Y., Zhang, H.R., Fan, J.W., Liang, M.J. and Wang, X.H., 2014. Two-phase subduction and subsequent collision defines the Paleotethyan tectonics of the southeastern Tibetan Plateau: Evidence from zircon U-Pb dating, geochemistry, and structural geology of the Sanjiang orogenic belt, southwest China. Bulletin, 126(11-12), pp.1654-1682.

Zhu, D.C., Mo, X.X., Zhao, Z.D., Niu, Y., Wang, L.Q., Chu, Q.H., Pan, G.T., Xu, J.F. and Zhou, C.Y., 2010. Presence of Permian extension-and arc-type magmatism in southern Tibet: paleogeographic implications. Bulletin, 122(7-8), pp.979-993.